



Enhanced microbial contribution to mineral-associated organic carbon accrual in drained wetlands: Beyond direct lignin-iron interactions

Chengzhu Liu^{a,b,c,1}, Simin Wang^{a,b,c,1}, Yunpeng Zhao^{a,b,c}, Ya Wang^{a,b,c}, Yiyun Wang^d,
Erxiang Zhu^{a,b}, Juan Jia^{a,b}, Zongguang Liu^{a,b,c}, Jin-Sheng He^{e,f}, Xiaojuan Feng^{a,b,c,*}

^a State Key Laboratory of Vegetation and Environmental Change, Institute of Botany, Chinese Academy of Sciences, Beijing, 100093, China

^b China National Botanical Garden, Beijing, 100093, China

^c University of Chinese Academy of Sciences, Beijing, 100049, China

^d East China Normal University, Shanghai, 200241, China

^e State Key Laboratory of Grassland Agro-ecosystems, College of Pastoral Agriculture Science and Technology, Lanzhou University, Lanzhou, 730000, China

^f Institute of Ecology, College of Urban and Environmental Sciences, Peking University, Beijing, 100871, China

ARTICLE INFO

Keywords:

Drainage

Soil organic carbon

Wetland

Mineral-associated organic carbon

Microbial-derived sugars

Lignin phenol

ABSTRACT

Drainage poses a major threat to the tremendous soil organic carbon (SOC) reservoir in wetlands. However, drainage-induced carbon loss may be mitigated by the accumulation of mineral-associated organic carbon (MAOC) via both microbial processes and iron (Fe)-organic matter (especially lignin) interactions, which remains under-investigated in wetlands. Here using a novel analytical approach, we quantitatively examined the response of MAOC to drainage and the driving mechanisms in four distinct wetlands. Contrary to the prevailing assumption, MAOC consisted a significant fraction (7%–91%) of wetland SOC, and increased with mineral-bound (microbial-dominated) sugars, but decreased with Fe-bound lignin phenols in SOC assessed after removal of reactive soil minerals. Furthermore, mineral-bound sugars increased with clay and reactive aluminum instead of Fe, and overrode Fe-bound lignin regarding contribution to MAOC after long-term drainage. These results indicate that microbial processes leading to microbial sugars accumulation played a prominent role in wetland MAOC accrual after long-term drainage, especially in soils rich in reactive Al and clay. Our study highlights the prevalent yet under-investigated microbial regulation on MAOC accrual in wetlands during long-term drainage. Given the large stock and persistence of MAOC in wetlands, its increase may partly compensate for particulate organic carbon loss during drainage, and may underpin wetland SOC stabilization in the long term.

1. Introduction

Wetlands cover 2% of the Earth's surface (Davidson et al., 2018), but store approximately one-third of soil carbon (ca. 600 Gt) globally (Zedler and Kercher, 2005; Yu et al., 2010). About 21% of the global wetland area (ca. 3.4 million km²) has been lost to artificial drainage mainly for agriculture between 1700 and 2020 (Fluet-Chouinard et al., 2023). Currently, the area of wetlands is still decreasing (by around 1% annually), potentially releasing about 0.5 Pg C annually, equivalent to 5% of the current anthropogenic carbon emissions (Evans et al., 2021; Temmink et al., 2022), thereby exacerbating global warming (Leifeld et al., 2019; Huang et al., 2021a). Hence, it is imperative to investigate

the influence of drainage on wetland carbon storage and stability to better understand and predict carbon-climate feedbacks under human disturbances.

Conventional wetland research largely focuses on total soil carbon stocks, which are assumed to be dominated by particulate organic carbon (POC) (Wang et al., 2014; Ji et al., 2020; Sokol et al., 2022) and to rapidly degrade upon oxygen exposure after drainage (Freeman et al., 2001; Fenner and Freeman, 2011). However, emerging studies have found that metal- or mineral-associated organic carbon (MAOC) constitutes 8–55% of soil organic carbon (SOC) in wetlands, and reactive minerals exert a strong influence on SOC stability (Zhao et al., 2019; Bai et al., 2021; Liu et al., 2021; Wang et al., 2021; Wei et al., 2022).

* Corresponding author. State Key Laboratory of Vegetation and Environmental Change, Institute of Botany, Chinese Academy of Sciences, Beijing, 100093, China.
E-mail address: xfeng@ibcas.ac.cn (X. Feng).

¹ Chengzhu Liu and Simin Wang contributed equally to this work.

Notably, MAOC may show contrasting responses to wetland drainage compared to POC, owing to increased protection by newly formed iron (Fe) (hydr)oxides (referred to as ‘direct Fe protection’ pathway in this paper; Wang et al., 2017), and/or enhanced microbial necromass accumulation as a result of increased microbial activity (referred to as ‘microbial processing’ pathway; Chen et al., 2021; Liu et al., 2021). Hence, the potential accrual of MAOC under wetland drainage may compensate for POC loss over long timescales (Liu et al., 2021). Given the much slower turnover of MAOC compared with POC (Lavalley et al., 2020; Heckman et al., 2022), MAOC dynamics and the regulating mechanisms are particularly worthy of investigation following drainage, which directly relate to wetland’s long-term carbon sink potentials. However, the prevalence, magnitude and regulating factors of the above two pathways regulating MAOC accumulation in wetlands remain unclear, constraining our capacity to predict and protect wetland carbon sinks.

The ‘direct Fe protection’ and ‘microbial processing’ pathways may sequester different SOC moieties during wetland drainage, and have distinct operating conditions. The former mainly involves sorption, complexation and/or co-precipitation of organic matter with reactive metal oxides during the oxidation of redox-sensitive metals and/or associated pH changes (Riedel et al., 2013; Chen et al., 2014; Hall et al., 2016; Patzner et al., 2020). As the most abundant redox-sensitive metals in natural wetlands, Fe plays a key role in this mechanism (Bhattacharyya et al., 2018; Huang et al., 2021b; Zhao et al., 2021), and exerts a high affinity to molecules rich in carboxyl, phenolic or aromatic carbon, such as lignin (Riedel et al., 2012, 2013; Coward et al., 2018). Hence, although metal oxides may protect a wide array of molecules, Fe-lignin interaction is proposed to be a key pathway contributing to SOC stabilization during the drainage of Fe-rich wetlands (Wang et al., 2017). However, the prevalence and significance of Fe-lignin interaction still await to be tested.

By comparison, the ‘microbial processing’ pathway invokes microbial conversion of labile substrates into microbial necromass, which (partly) stabilizes as MAOC in the soil due to microbe’s close association with mineral surfaces (Cotrufo et al., 2013; Liang et al., 2017; Sokol et al., 2019). This mechanism, while being extensively examined in upland soils (Ye et al., 2018; Sokol and Bradford, 2019; Sokol et al., 2022), is under-investigated in wetlands due to anaerobic conditions inhibiting microbial activity (Jia et al., 2020; Chen et al., 2021; Dao et al., 2022). However, wetland drainage may greatly enhance microbial activity and microbial contribution to MAOC, as is reflected by the accumulation of non-cellulosic sugars (abbreviated as ‘sugars’ in this paper; Liu et al., 2021) that have considerable contributions from microbes (Kögel-Knabner, 2002; Gunina and Kuzyakov, 2015). Compared with lignin, sugars are equally (if not more) abundant in wetlands (Younes et al., 2017; Jia et al., 2020), but show preferential associations with aluminosilicate clays and aluminum (Al) (hydr)oxides relative to Fe (hydr)oxides, especially those derived from microbes (Kiem and Kögel-Knabner, 2003; Kopittke et al., 2018; Creamer et al., 2019; Dao et al., 2022). Hence, comparing Fe-bound lignin vs. mineral-bound (microbial) sugars may delineate the relative importance and regulating factors of ‘direct Fe protection (of lignin)’ vs. ‘microbial processing’ pathways governing MAOC dynamics during wetland drainage.

Here we develop a novel analytical approach to quantify mineral-bound sugars by combining mineral dissolution method with biomarker analysis. Reactive Fe and Al that play a key role in SOC preservation in wetlands (Zhao et al., 2019; Anthony and Silver, 2020; Bai et al., 2021) are first dissolved by oxalate pretreatment, with mineral-bound sugars (in the oxalate extracts) and non-mineral-bound sugars (in the soil residues) subjected to hydrolysis by trifluoroacetic acid (TFA). We also adopt a previously used method to quantify Fe-bound lignin phenols in wetland soils rich in reactive Fe, which exposes ‘hidden’ lignin to the cuperic oxide (CuO) oxidation after removal of reactive Fe (Wang et al., 2017).

Using these analytical methods, we compare changes in mineral-

bound sugars vs. Fe-bound lignin phenols in relation to MAOC variations in four typical wetlands of China that experienced artificial drainage of various durations. These wetlands include a *Sphagnum*-dominated nutrient-poor bog and three nutrient-rich fens dominated by *Carex* with contrasting hydrological and edaphic characteristics, allowing us to clarify the relative importance and regulating factors of the ‘direct Fe protection of lignin’ and ‘microbial processing’ pathways regulating MAOC dynamics during wetland drainage. Given that drainage generally stimulates microbial activity in wetlands, we hypothesize that (1) contrary to the common assumption of decreased carbon accumulation after wetland drainage, MAOC increases in SOC due to ‘microbial processing’ and ‘direct Fe protection of lignin’ pathways promoting the preservation of mineral-associated moieties; (2) ‘microbial processing’ predominates MAOC increases after long-term drainage such that mineral-bound sugars override Fe-bound lignin phenols, especially in soils rich in reactive Al and clay; however, (3) ‘direct Fe protection of lignin’ may be important in wetlands showing increased Fe reactivity.

2. Materials and methods

2.1. Study sites and soil sampling

To investigate the response of MAOC and mineral-bound carbon components to drainage in different types of wetlands, we selected a typical bog (Dajiuhu) and two fens (Hongyuan, Fuyuan) that have experienced decades of artificial drainage in China (details in Fig. 1). Dajiuhu is a bog located in a closed subalpine basin (110°00′ E, 31°29′ N) in Mt. Shen-Nong-Jia, Hubei Province. Fuyuan and Hongyuan are fens located in the Sanjiang Plain (134°32′ E, 48°3′ N) and the Zoige wetland on the Qinghai-Tibetan Plateau (102°39′ E, 33°6′ N), respectively. Soils were sampled from replicated plots (n = 4) in the waterlogged and drained areas of these wetlands in August and September 2017. The aboveground biomass and plant debris were removed before soil sampling by corer (diameter of 7 cm, depth of 40 cm). Soil cores were sliced into four depths at 10-cm intervals, cooled during transport to the laboratory, freeze-dried, and sieved (<2 mm) afterwards.

In addition, soils subjected to a mesocosm water-table manipulation experiment from the Haibei wetland, located on the northeastern edge of the Qinghai-Tibetan Plateau (101°20′ E, 37°35′ N), were also included to examine the relatively short-term responses of MAOC (details in Fig. 1). The experiment consisted of duplicated control (waterlogged) and drainage (water-table of -20 cm) treatments (n = 4) in intact soil tanks (60 cm × 60 cm × 65 cm). In September 2013, after 27 months of experiment, soils in both waterlogged and drained treatments were sampled using soil corer (5 cm in diameter), and sliced into different depth sections. Details of the manipulation experiment and sampling were described in Wang et al. (2017). Three depths were chosen for this study (4–10, 10–20, and 30–40 cm), while the topmost layer (0–4 cm) was not included due to paucity of soil. Basic soil properties and lignin phenols were reported in Wang et al. (2017), while MAOC and mineral-bound sugars were analyzed in this study.

2.2. Soil physicochemical analysis

Plant roots were picked out from freeze-dried soils and weighed as root mass. Soil ‘core density’ was calculated based on the volume and dry mass of each soil core (Liu et al., 2021), given difficulties of making bulk density measurements in wetlands. The above parameters were unfortunately not collected for the mesocosm experiment in Haibei. Soil pH was measured at a soil:water ratio of 1:15 (w:v). Dithionite-extractable Fe (Fe_d), including both short-range-ordered (SRO) and some crystalline Fe, was extracted using the citrate-bicarbonate-dithionite method (Lalonde et al., 2012). Oxalate-extractable Fe and Al (Fe_o and Al_o; representing SRO and organically complexed Fe and Al) were extracted using 0.2 M

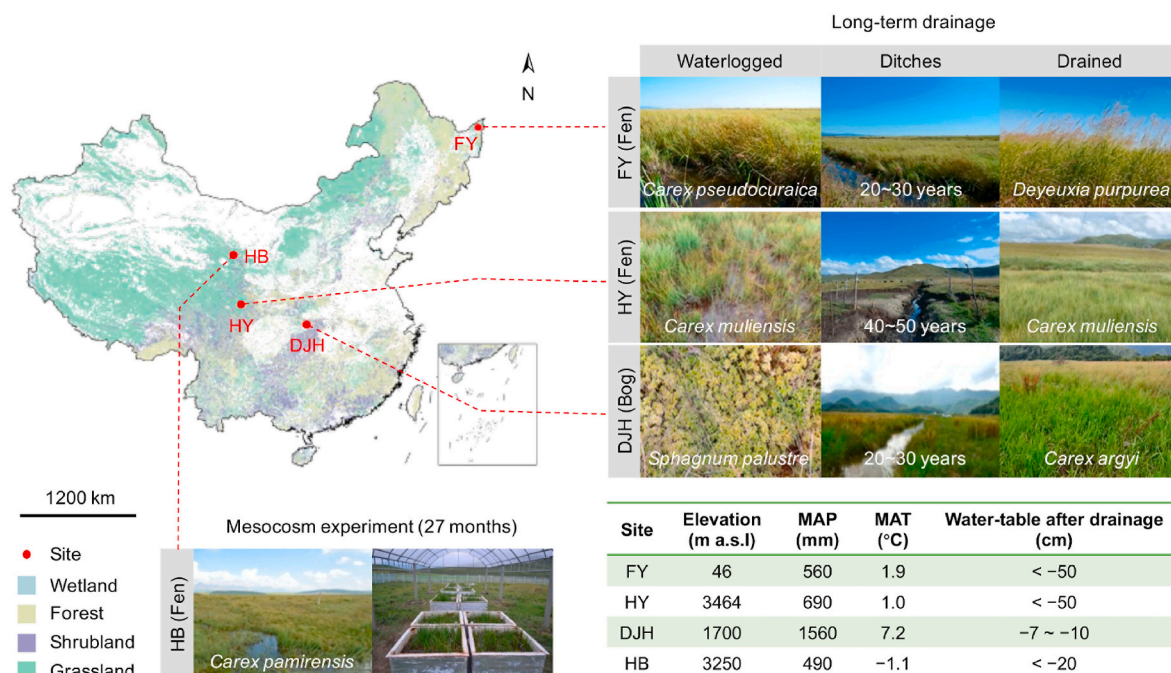


Fig. 1. Distribution and pictures of the investigated wetland sites in China, including a typical bog (Dajiuhu, DJH) and two fens (Hongyuan, HY; Fuyuan, FY) that have experienced decades of artificial drainage as well as a mesocosm water-table manipulation experiment (Haibei, HB). The vegetation distribution map is based on China's vegetation map (1:1000000). MAP, mean annual precipitation; MAT, mean annual temperature.

ammonium oxalate at pH 3 for 4 h (Wang et al., 2017; Bhattacharyya et al., 2018; Anthony and Silver, 2020; details in Supplementary Text S1). Both Fe and Al were quantified on an inductively coupled plasma-optical emission spectrometer (ICP-OES; iCAP 6300, Thermo Scientific, USA). The ratio of $Fe_o:Fe_d$ was used to infer the reactivity of Fe (hydr)oxides (Blume and Schwertmann, 1969; Hall and Thompson, 2018). Soil texture was determined using a Laser Particle Size Analyzer (Mastersizer, 2000) following the laser diffraction method (Ryzak and Bieganski, 2011; details in Text S1). The SOC and total N contents were determined on an elemental analyzer (Vario EL III; Elementar, Hanau, Germany), after removal of inorganic carbon by acidification (for SOC; Harris et al., 2001). Note that data of pH, SOC, Fe, Al in Dajiuhu, Fuyuan and Hongyuan, as well as clay in Dajiuhu and Hongyuan (10–20 and 30–40 cm) are from our previous studies (Liu et al., 2021; Wang et al., 2023); properties of Haibei soils are from Wang et al. (2017) except clay and SOC contents. For Haibei, clay contents, pH and SOC were measured for bulk soils, whereas other properties were measured for the <53 μ m fraction.

2.3. Analysis of MAOC and Fe-bound organic carbon (Fe-bound OC)

Mineral-associated organic matter (MAOM; density of 1.6 g cm⁻³ and size <53 μ m) was isolated from dried soils using a method modified from Griepentrog et al. (2014) involving sequential fractionation by density (using sodium polytungstate solution) and size (details in Text S2). The MAOC contents were analyzed on an elemental analyzer as described previously, and converted into contents (in the units of mg g⁻¹ soil) or MAOC percentage (in bulk SOC), given the weight percentage of each fraction. As an important contributor to MAOC, OC associated with reactive Fe (Fe-bound OC) was examined using the citrate–bicarbonate–dithionite method (Lalonde et al., 2012), with another aliquot of dry soil extracted with sodium chloride (NaCl) as a control. Fe-bound OC was calculated as the OC difference of NaCl- and dithionite-treated soil residues, and expressed in percentage relative to bulk SOC (details in the Text S2). The MAOM contents were determined for two layers (10–20 and 30–40 cm) of Dajiuhu and Hongyuan soils in our previous study (Liu et al., 2021).

2.4. Analysis of Fe-bound lignin phenols and mineral-bound sugars

Fe-bound lignin phenols and mineral-bound sugars were quantified by biomarker analysis following dithionite and oxalate pretreatment to remove protection by reactive minerals, respectively (Fig. S1). A series of supplementary analyses were conducted to validate the analytical methods (details in Text S3, Table S1, Fig. S2). Briefly, oxalate is effective in extracting SRO Al (hydr)oxides and aluminosilicates such as allophane and imogolite, and in partially releasing Al from crystalline silicates (Parfitt and Childs, 1988; Kramer et al., 2012; Rennert, 2019; Hall and Thompson, 2021), thereby liberating sugars that strongly associate with reactive Al in soils (Creamer et al., 2019; Han et al., 2021; Dao et al., 2022). By comparison, dithionite dissolves SRO Fe (hydr)oxides and a minor portion of poorly crystalline aluminosilicates (Dahlgren, 1994; Rennert, 2019), thereby exposing 'hidden' lignin that strongly associate with reactive Fe (Riedel et al., 2012; Wang et al., 2017). Based on these rationales and preliminary tests (Fig. S2), dithionite pretreatment coupled with CuO oxidation (modified after Wang et al., 2017) and oxalate pretreatment coupled with TFA hydrolysis (Zhang et al., 2007) were used to analyze Fe-bound lignin phenols and mineral-bound sugars in this study, respectively.

Briefly, after soil treatment by the citrate–bicarbonate–dithionite method (Lalonde et al., 2012), the supernatant (i.e., dithionite solution) containing dissolved and Fe-bound lignin was acidified to pH < 2 to maintain Fe in the solution and kept in the dark at 4 °C for 2 days to allow the oxidation of dithionite. Precipitates formed at this step likely due to coagulation of organic matter with inorganics and were recovered using centrifugation, followed by rinsing with acidified MilliQ water (pH < 2) three times (referred to as 'dithionite precipitates'). Dissolved lignin in the supernatant was concentrated using C₁₈ solid phase extraction (SPE) cartridges (Louchouart et al., 2000; Spencer et al., 2010) and eluted with methanol (referred to as 'dithionite liquids'). Lignin phenols in the dithionite-treated soil residues, dithionite solution (including both precipitates and liquids) as well as the original bulk soils were isolated using CuO oxidation (Lee et al., 2019; Text S3). For sugars, the oxalate-treated soil residues (containing non-mineral-bound sugars) and the filtered oxalate liquids (containing mineral-bound sugars) were

subjected to TFA hydrolysis (Text S3.3). Eight sugars were identified, including glucose, galactose, arabinose, xylose, mannose, rhamnose, ribose, and fucose.

Assuming that dithionite pretreatment exposed Fe-bound lignin phenols that were originally not amenable to CuO oxidation, we estimated Fe-bound lignin phenols as (Wang et al., 2017):

$$\text{Fe-bound lignin phenols} = (\Sigma_r + \Sigma_p + \Sigma_{\text{liquid}}) - \Sigma_{\text{soil}} \quad (1)$$

where Σ_r , Σ_p , Σ_{liquid} and Σ_{soil} represent lignin phenols in the dithionite-treated soil residues, precipitates and liquids of the dithionite solution, and bulk soils, respectively (all normalized to the original soil mass). It should be mentioned that cinnamyl phenols were subjected to loss during dithionite treatment, likely due to a poor solid-phase extraction efficiency for the more soluble cinnamyl phenols from the aqueous phase and/or potential Fenton-like reactions with the more degradable cinnamyl phenols (Hedges et al., 1985; Feng and Simpson, 2008). Hence, cinnamyl phenols were excluded in the calculation of Fe-bound lignin phenols as tested in Wang et al. (2017).

We assumed that mineral-bound sugars were released into the liquid phase during oxalate pretreatment. Therefore, sugars in the oxalate liquids and oxalate-treated soil residues represented mineral-bound sugars and non-bound sugars, respectively. To avoid overestimation by inclusion of water-extractable sugars in the oxalate liquids, we used water-extracted soils to assess responses of mineral-bound sugars to wetland drainage (Fig. S1).

The ratio of galactose + mannose to arabinose + xylose (GM/AX) was calculated to infer microbial vs. plant contributions to sugars, as is commonly used in the literature (Kögel-Knabner, 2002; Gunina and Kuzakov, 2015). The GM/AX ratio of the aboveground and belowground tissues of the dominant plant species was also analyzed for reference (details in Table S2). Due to the labor-intensive nature of the analyses, mineral-bound sugars and Fe-bound lignin phenols were only examined at selected depths, including two layers (10–20 and 30–40 cm) for all soils and the surface layer for Dajiuhu (0–10 cm) and Haibei (4–10 cm). One Dajiuhu sample, one Fuyuan sample and one Haibei sample were lost during biomarker extraction. The Fe and Al species, Fe-bound OC and biomarkers were analyzed for MAOM of Haibei soils in our previous study (Wang et al., 2017).

To compare the relative contribution of different mineral-bound components to MAOC, we calculated MAOC-normalized contents of Fe-bound lignin phenol-C and mineral-bound sugar-C based on the C content of each compound. Given that lignin phenols isolated by CuO oxidation do not account for all lignin-derived C (Kögel-Knabner, 2002), we roughly estimated Fe-protected lignin-C based on the ratio of lignin phenols to Klason lignin isolated from the same plant materials (0.2 ± 0.01) (Ma et al., 2018) and C content of lignin macromolecules (60%; Souto et al., 2018):

$$\Lambda_{\text{lignin-C}} = (\Lambda_{\text{lignin phenols}} \times 60\%) / 0.2 \quad (2)$$

where $\Lambda_{\text{lignin-C}}$ and $\Lambda_{\text{lignin phenols}}$ represent SOC-normalized contents of lignin-C and lignin phenols, respectively.

2.5. Statistics

All statistical analyses were conducted using R version 3.6.0 (R Core Team, 2018). Two-way ANOVA was used to examine the effects of treatment (waterlogged vs. drained) and soil depth on the investigated parameters for each site, followed by one-way ANOVA to examine the effects of treatment in the presence of interactive effects. To compare responses to drainage among different wetlands, the response ratio (RR) of drained relative to waterlogged plots across all examined depths was calculated for each site (Hedges et al., 1999):

$$\text{RR} = \ln \left(\frac{X_i}{X_c} \right) = \ln(X_i) - \ln(X_c) \quad (3)$$

where X_i and X_c are the means for individual depth at each site in drained and waterlogged soils, respectively. A positive value of RR indicated an increase of the examined variable in the drained than waterlogged soils, and *vice versa*. Given different variances of the calculated RR for different depths at each site, the weight of each depth was estimated based on the reciprocal of the variance for individual RRs. To consolidate site-specific responses, we further evaluated depth-weighted response (RR_{++}) following Hedges et al. (1999) by weighting the RR of individual depths with the inverse variance (see details in Text S4) for each site, respectively. If the 95% confidence interval did not overlap with zero, the drainage response was considered to be significant.

Linear mixed effects models were used to analyze the fixed effects of treatment (waterlogged vs. drained), fraction (oxalate liquids, soil residues, bulk soils), and their interactions on GM/AX ratios, using the *lme* function in R “nlme” package (Pinheiro et al., 2020). In the models, site and depth served as random factors. Subsequently, we performed multiple comparisons with Tukey’s test, using the *glht* function in R “multcomp” package (Hothorn et al., 2008), to test differences of GM/AX ratios among three fractions (oxalate liquids, soil residues, bulk soils) ($p < 0.05$). In the presence of interactive effect, multiple comparisons were conducted for the waterlogged and drained soils, respectively. Using the same approach, we conducted linear mixed effects models and multiple comparisons to analyze the fixed effects of treatment (waterlogged vs. drained), mineral-bound components (sugars, lignin phenols, macromolecular lignin), and their interactions on the MAOC-normalized concentration of mineral-bound components.

Redundancy analysis (RDA) was performed to assess the covariance of Fe-bound lignin phenols and mineral-bound sugars with their potential influencing factors, including soil properties (SOC:N and pH), mineral properties (clay contents, $\text{Fe}_0:\text{Fe}_d$, Al_0), MAOC and Fe-bound OC. The original data were normalized into the range of [0, 1] before RDA analysis. Differences and correlations were considered to be significant at a level of $p < 0.05$. Spearman’s correlation was used to test relationships of the investigated parameters (non-normally distributed). Properties of Haibei samples were mainly based on MAOM instead of bulk soils in our previous study and hence not included in the correlation or RDA analysis.

3. Results

3.1. Changes of wetland soil physicochemical properties after drainage

The results of two-way ANOVA showed that drainage-induced changes of soil properties were mostly consistent along the examined depths or pronounced in certain layers at the same site (Fig. S3). Briefly, long-term drainage had a significant influence on most layers of Dajiuhu and Fuyuan, but did not change soil properties at 20–40 cm in Hongyuan (Fig. S3). Soil properties did not change after short-term drainage in Haibei, except for decreasing soil pH at 4–20 cm. To consolidate site-specific responses, we calculated weighted RR (RR_{++}) across all examined depths for each site. Based on the RR_{++} , drainage increased soil pH relative to the waterlogged site due to the decline of acid-producing *Sphagnum* in Dajiuhu ($p < 0.05$), but decreased soil pH in Fuyuan, Hongyuan, and Haibei wetlands ($p < 0.05$; Fig. 2a), likely due to Fe oxidation-induced proton release during ferric iron [Fe(III)] hydrolysis (Wang et al., 2017). Long-term drainage decreased both Fe_0 and Fe_d in Fuyuan and Hongyuan, but increased Fe_d in Dajiuhu ($p < 0.05$, Fig. 2b and c). Accordingly, Fe reactivity, indicated by the $\text{Fe}_0:\text{Fe}_d$ ratio, decreased after drainage in Dajiuhu, but increased slightly in Hongyuan ($p < 0.05$; Fig. 2d). Drainage increased Al_0 in Fuyuan and Hongyuan, but decreased Al_0 in Haibei ($p < 0.05$; Fig. 2e). Long-term drainage also increased soil core density in Dajiuhu with reduced root mass, but decreased core density in Hongyuan and Fuyuan ($p < 0.05$; Figs. S5a and b). Clay contents increased in both Dajiuhu and Fuyuan after drainage,

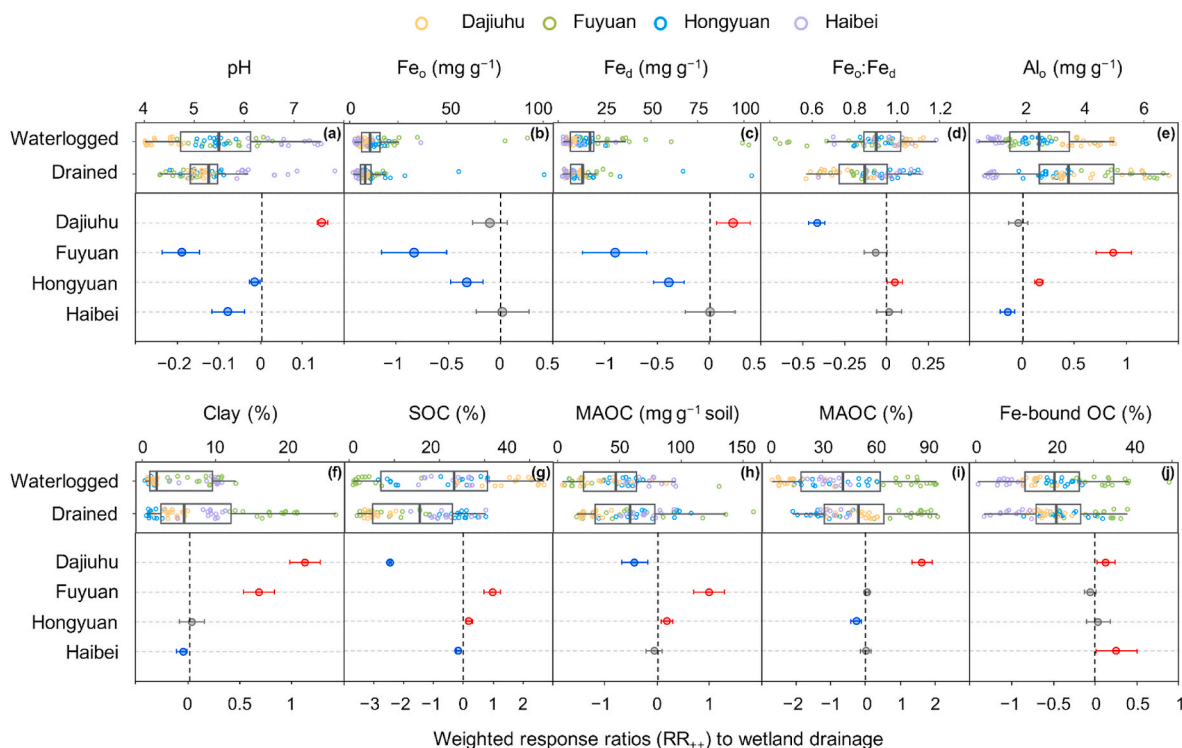


Fig. 2. Comparison of raw data and depth-weighted response ratios (RR_{++}) of soil parameters in the drained relative to waterlogged soils for each wetland. (a) Soil pH; (b) oxalate-extractable iron (Fe_o); (c) dithionite-extractable Fe (Fe_d); (d) ratios of $Fe_o:Fe_d$; (e) oxalate-extractable aluminum (Al_o); (f) clay contents; (g) soil organic carbon (SOC); (h) contents of mineral-associated organic carbon (MAOC); (i) percentage of MAOC in SOC; (j) Fe-bound organic carbon (OC). Solid line in the box marks the mean of each dataset. The upper and lower ends of boxes denote the 0.25 and 0.75 percentiles, respectively. The upper and lower whisker caps denote the maximum and minimum values, respectively. Hollow dots denote raw data in the boxplots. Solid dots represent values of RR_{++} and bars represent the 95% CIs (details in SI). If the 95% CI value of RR_{++} does not overlap with zero, the response is considered to be significant. The red, blue and grey dots denote significant increase, decrease and no-change, respectively. Note that data of pH, SOC, Fe, Al in Dajiuhu, Fuyuan and Hongyuan, as well as clay and MAOC in Dajiuhu and Hongyuan (10–20 and 30–40 cm) are from our previous studies (Liu et al., 2021; Wang et al., 2023); properties of Haibei soils are from Wang et al. (2017) except clay and SOC contents. For Haibei, clay contents, pH, SOC and MAOC were measured for bulk soils, whereas other properties were measured for the $<53 \mu m$ fraction.

but decreased in Haibei ($p < 0.05$), and did not change in Hongyuan ($p > 0.05$; Fig. 2f).

3.2. Changes in SOC, MAOC and Fe-bound OC

Long-term drainage considerably decreased SOC contents in Dajiuhu, but increased those in Fuyuan and Hongyuan ($p < 0.05$; Fig. 2g). Drainage decreased SOC:N in Dajiuhu, Hongyuan, and Fuyuan ($p < 0.05$; Fig. S5c). Contents of MAOC showed a similar changing pattern as SOC after long-term drainage ($p < 0.05$; Fig. 2h). However, MAOC percentage in SOC increased in Dajiuhu, decreased in Hongyuan ($p < 0.05$), and did not change in Fuyuan ($p > 0.05$; Fig. 2i). The percentage of Fe-bound OC in SOC increased in Dajiuhu ($p < 0.05$), and did not change in Fuyuan and Hongyuan after drainage ($p > 0.05$; Fig. 2j). By comparison, the relatively short-term drainage decreased SOC, increased Fe-bound OC percentage in Haibei ($p < 0.05$), and had no significant influence on MAOC or SOC:N ($p > 0.05$; Fig. 2g–j and S5c).

3.3. Responses of Fe-bound lignin phenols and mineral-bound sugars to drainage

Drainage decreased SOC-normalized contents of lignin phenols in the bulk soil of Dajiuhu, Fuyuan, Hongyuan and Haibei ($<53 \mu m$ fraction for Haibei) relative to the waterlogged sites ($p < 0.05$; Fig. 3a and b, Fig. S4a). Removal of reactive Fe by dithionite pretreatment released up to 66% of Fe-bound lignin phenols relative to lignin phenols in the bulk soils. Negative values of Fe-bound lignin phenols were observed in 15 out of 55 analyzed soil samples in this study, which had relatively low SOC contents (Fig. S6a), suggesting loss of soluble phenols during the

dithionite pretreatment (Wang et al., 2017). Hence, Fe-bound lignin phenols may be underestimated, but comparisons between treatments within the same wetland (with similar range of SOC and mineralogy) should be valid. The SOC-normalized contents of Fe-bound lignin phenols decreased in Dajiuhu but did not change in Fuyuan and Hongyuan (Fig. 3c and d). Although the RR_{++} of Fe-bound lignin phenols did not change in Haibei (Fig. 3c and d), two-way ANOVA indicated a significant increase in the SOC-normalized content of Fe-bound lignin phenols in the air-exposed layers (4–20 cm; $p < 0.05$; Fig. S4b), as reported by Wang et al. (2017).

By comparison, SOC-normalized contents of total sugars (summation of oxalate liquids and soil residues) increased in both Dajiuhu and Fuyuan after drainage ($p < 0.05$), but did not change in Hongyuan or Haibei ($p > 0.05$; Fig. 3a, b and S4c). Oxalate pretreatment liberated 4%–39% of mineral-bound sugars relative to total sugars in all soils. The SOC-normalized contents of mineral-bound sugars also increased in Dajiuhu and Fuyuan after drainage ($p < 0.05$; Fig. 3c, d and S4d), but did not change in Hongyuan or Haibei ($p > 0.05$). Moreover, the GM/AX ratio increased in both liquid extracts and soil residues of the oxalate treatment after drainage relative to waterlogged samples ($p < 0.05$), and was much higher in the ‘liquid’ than ‘residue’ fraction ($p < 0.05$; Fig. 4a). These results suggest that microbial-derived sugars increased after drainage, and were preferentially associated with minerals compared with plant-derived sugars.

To compare the relative contribution of Fe-bound lignin vs. mineral-bound sugars to MAOC, we calculated using Equation (2) that although Fe-bound lignin phenol-C had comparable contents ($11.1 \pm 2.2 \text{ mg g}^{-1}$ MAOC; mean \pm SE) to mineral-bound sugar-C ($28.2 \pm 4.4 \text{ mg g}^{-1}$ MAOC) in waterlogged soils ($p > 0.05$), Fe-bound lignin-C was much

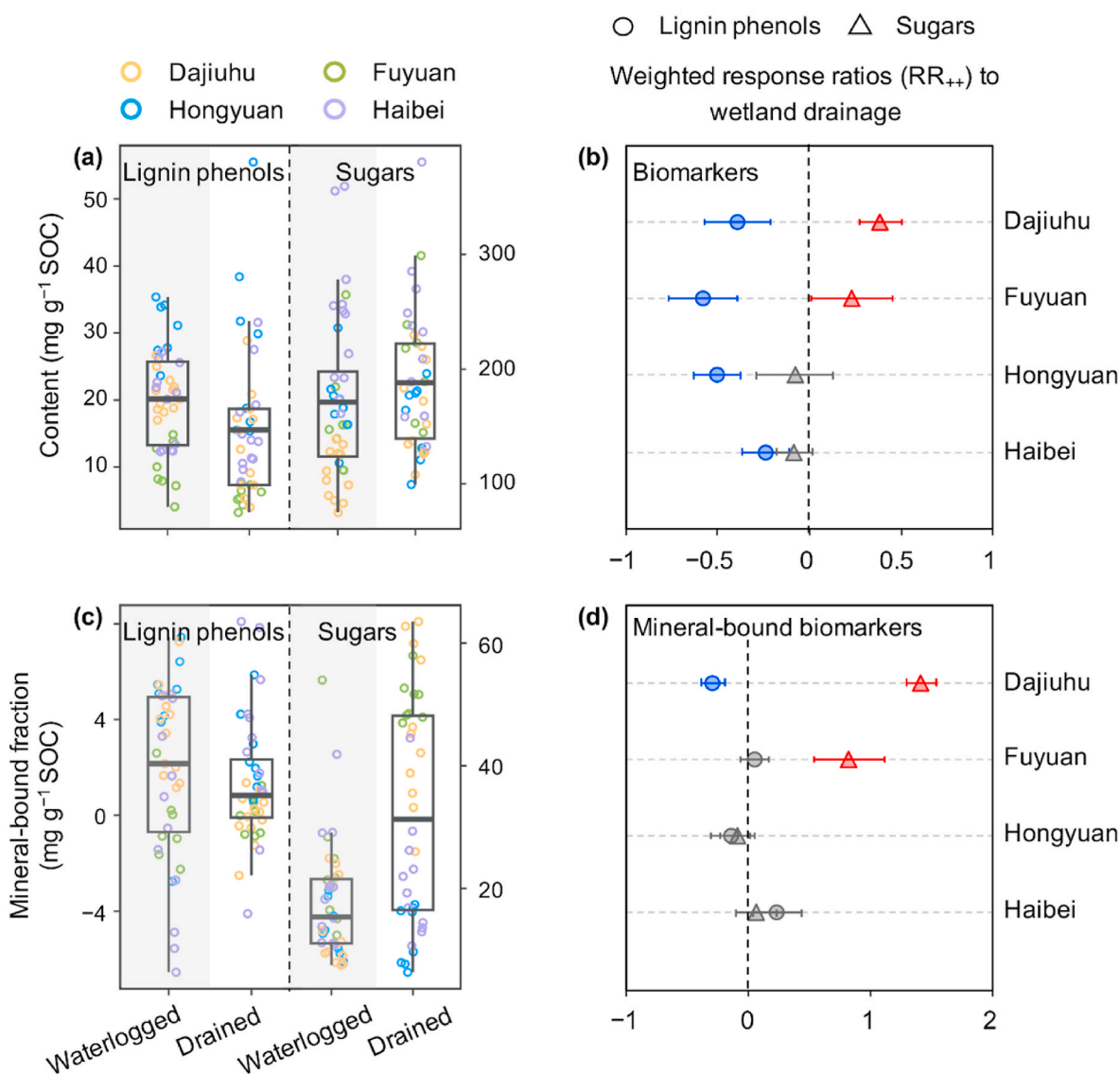


Fig. 3. Comparison of raw data (a, c) and depth-weighted response ratios (RR₊₊) of lignin phenols and sugars in the drained relative to waterlogged soils for each wetland (b, d): soil organic carbon (SOC)-normalized contents in bulk soils (a) and the respective RR₊₊ (b); contents of Fe-bound lignin phenols and mineral-bound sugars (c) and the respective RR₊₊ (d). Symbols are explained in the caption of Fig. 2. Note that data of Fe-bound lignin phenols in Haibei are from Wang et al. (2017) based on the <53 μm fraction, while the other analysis was based on bulk soils.

higher ($58.4 \pm 11.8 \text{ mg g}^{-1} \text{ MAOC}$; $p < 0.05$; Fig. 4b), considering that lignin phenols only represented a small fraction (~20%) of the macromolecular lignin (Ma et al., 2018). Notably, drainage significantly decreased the MAOC-normalized contents of Fe-bound lignin-C ($2.2 \pm 1.4 \text{ mg g}^{-1} \text{ MAOC}$) and lignin phenol-C ($0.4 \pm 0.3 \text{ mg g}^{-1} \text{ MAOC}$), but did not change those of mineral-bound sugar-C ($29.8 \pm 1.9 \text{ mg g}^{-1} \text{ MAOC}$; $p < 0.05$), resulting in higher contents of mineral-bound sugar-C than Fe-bound lignin-C or lignin phenol-C in the MAOC of drained soils ($p < 0.05$). These results indicate that Fe-bound lignin contributed more to MAOC in the waterlogged soils, while mineral-bound sugars overrode Fe-bound lignin in MAOC after drainage.

3.4. Influencing factors on mineral-bound components

To reveal the co-variance of Fe-bound lignin phenols and mineral-bound sugars with environmental variables including MAOC, an RDA model was performed based on soils experiencing long-term drainage (Dajihu, Fuyuan and Hongyuan; Fig. 4c). The two axes of the RDA model explained nearly 76% of the variances in mineral-bound

components ($n = 52$, due to loss of several samples). Fe-bound lignin phenols aligned closely with SOC:N and Fe_o:Fe_d ratios, while mineral-bound sugars aligned closely with clay, Al_o, MAOC and Fe-bound OC, on the opposite side of the x-axis (Fig. 4c). This result suggests different environmental controls on Fe-bound lignin phenols vs. mineral-bound sugars and their varied influences on MAOC and Fe-bound OC.

Further correlation analysis confirmed that the percentages of MAOC and Fe-bound OC in SOC were negatively correlated with the SOC-normalized content of Fe-bound lignin phenols ($r = -0.66$ and -0.33 , respectively; $p < 0.05$), but positively correlated with that of mineral-bound sugars ($r = 0.64$ and 0.32 , respectively; $p < 0.05$; Fig. 5a–d). Moreover, Fe-bound lignin phenols were positively correlated with Fe_o:Fe_d ($r = 0.64$; $p < 0.001$) and SOC:N ($r = 0.66$; $p < 0.001$), and negatively correlated with clay contents ($r = -0.55$; $p < 0.001$; Fig. 5e–l). A positive correlation between Fe-bound lignin phenols and Fe_o:Fe_d was also observed in the short-term drainage of Haibei soils ($r = 0.42$; $p < 0.05$; Fig. S6b). In contrast, mineral-bound sugars were positively correlated with clay ($r = 0.71$; $p < 0.001$) and Al_o contents ($r = 0.34$; $p < 0.05$), and negatively correlated with SOC:N ratios ($r = -0.79$; $p <$

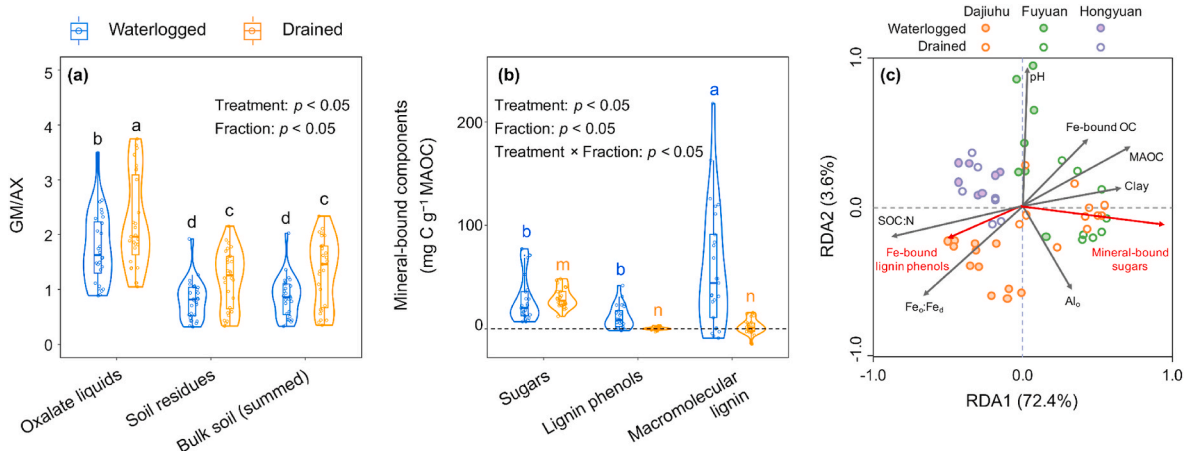


Fig. 4. Composition and variation of mineral-bound biomarkers in relation to mineral-associated organic carbon (MAOC): (a) ratios of galactose + mannose to arabinose + xylose (GM/AX) in the mineral-bound (oxalate liquids), non-bound fractions (soil residues) and bulk soils (oxalate liquids + soil residues); (b) contents of mineral-bound sugar-C, Fe-bound lignin phenol-C and Fe-bound macromolecular lignin-C after normalization to MAOC; (c) ordination biplot diagram for the redundancy analysis (RDA) displaying the effect of environmental factors on the variance of Fe-bound lignin phenols and mineral-bound sugars. The percentage reported in the RDA axis represent the amount of explained variance (72.4% for RDA1 and 3.6% for RDA2). Variance explained by all variables are 76%. The contents of macromolecular lignin-C are estimated based on the ratio of lignin phenols to Klason lignin isolated from the same plant materials and C content of lignin macromolecules (details in Methods). Data in (a) and (b) were analyzed using linear mixed models with site and depth as random factors. Tukey's test was used for multiple comparisons. In the presence of interactive effect, separate multiple comparisons were performed for the waterlogged and drained soils. Lowercase letters on top of the violins indicate significant differences among the groups ($p < 0.05$). Shapes of the violin represent distribution patterns of the corresponding data. Solid line in the box marks the median of each dataset. The upper and lower ends of boxes denote the 0.25 and 0.75 percentiles, respectively. The upper and lower whisker caps denote the maximum and the minimum values, respectively. Dots denote raw data. Note that outliers are deleted in (b). Abbreviations in (c) are defined in Fig. 2. Red arrows represent dependent variables; grey arrows represent environmental factors; blue and orange dots represent data of waterlogged and drained soils, respectively (c). Note that Haibei data (based on the $<53 \mu\text{m}$ fraction) are not included.

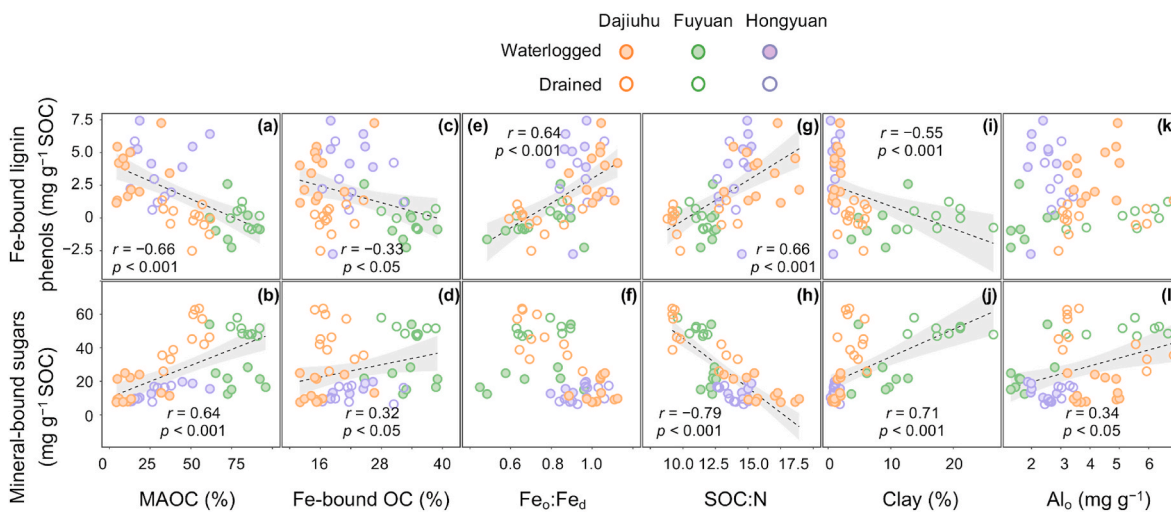


Fig. 5. Relationships of Fe-bound lignin phenols and mineral-bound sugars with major influencing variables. (a–b) MAOC (%); (c–d) Fe-bound OC (%); (e–f) ratios of $\text{Fe}_o:\text{Fe}_d$; (g–h) ratios of soil organic carbon to nitrogen (SOC:N); (i–j) clay contents; (k–l) Al_o . DJH, FY, HY and HB indicate wetlands at Dajiuhu, Fuyuan, Hongyuan and Haibei, respectively. Black dotted lines represent significant Spearman correlations. Shaded areas represent the 95% confidence intervals for the regression lines. Abbreviations are defined in Fig. 4. Note that Haibei data (based on the $<53 \mu\text{m}$ fraction) are not included.

0.001; Fig. 5e–l).

4. Discussion

Contrary to the prevailing assumption that wetland SOC mainly consists of POC (Wang et al., 2014; Sokol et al., 2022) and is subjected to loss after drainage (Turetsky et al., 2011; Lu et al., 2021), our study shows that MAOC accounted for 7%–91% of SOC in the waterlogged and drained soils across four distinct wetlands, and that MAOC content increased together with SOC after long-term drainage in Hongyuan and Fuyuan (Fig. 2g–i and S3f–h). Despite declined SOC and MAOC contents

in the drained bog (Dajiuhu), the proportion of MAOC in SOC increased, whereas the relatively short-term drainage slightly decreased SOC, increased Fe-bound OC, but did not change MAOC in Haibei. These results partly support Hypothesis 1, and highlight the importance of MAOC in wetland SOC stocks and in mediating SOC variations after long-term drainage. As MAOC turns over more slowly than POC (Lavallee et al., 2020; Heckman et al., 2022), the dynamics and accumulation potentials of MAOC may underpin wetland SOC stabilization and its long-term trajectory after drainage (Georgiou et al., 2022).

Given the crucial role of MAOC in wetland SOC accumulation after drainage, we attempt to compare the relative influence of 'microbial

processing' and 'direct Fe protection of lignin' on MAOC accrual by quantifying the response of mineral-bound (microbial) sugars vs. Fe-bound lignin phenols to drainage, using modified methods combining mineral dissolution and biomarker analyses (Fig. S1). We show that mineral-bound sugars (in the oxalate liquid extracts) had high ratios of GM/AX (2.2 ± 0.1) compared to plant tissues of the dominant wetland species (0.3 ± 0.05 ; except *Sphagnum*; Table S2) (Oades, 1984; Rumpel et al., 2010; Gunina and Kuzyakov, 2015; Liu et al., 2021), especially after drainage (Fig. 4a), indicating a dominant microbial contribution to mineral-bound sugars. Moreover, SOC-normalized contents of mineral-bound sugars increased with soil clay and Al_o contents rather than Fe content or reactivity (i.e., $Fe_o:Fe_d$; Fig. 5), implying the strong association of (microbial-derived) sugars with aluminosilicate clays, SRO Al (hydr)oxides, and/or organically complexed Al (Mikutta et al., 2009; Han et al., 2021; Dao et al., 2022). In contrast, SOC-normalized contents of Fe-bound lignin phenols increased with $Fe_o:Fe_d$ in all wetlands subjected to both long-term and short-term drainage (Fig. 5e and S6b), and decreased with clay content (Fig. 5i), reflecting the high affinity of lignin moieties to reactive Fe (hydr)oxides rather than clay (Kaiser, 2003; Riedel et al., 2012; Hall et al., 2016; Wang et al., 2017). These results confirm our expectation that if drainage promotes MAOM formation via 'microbial processing' pathway, we would observe an increase in mineral-bound (microbial) sugars and their contribution to MAOM. If 'direct Fe protection of lignin' works, Fe-bound lignin phenols and their contribution to MAOM would increase after drainage. Although it is challenging to trace processes associated with the two pathways after long-term drainage, we could delineate the relative importance of these pathways in governing MAOC dynamics by comparing the contributions of the two mineral-bound components to MAOC.

Using this approach, we find that consistent with Hypothesis 2, 'microbial processing' played a prominent role in MAOC accumulation during the long-term drainage of wetlands, as is reflected in two aspects: (i) both MAOC and Fe-bound OC increased with mineral-bound sugar contents, but decreased with Fe-bound lignin phenol contents in SOC (Fig. 4c and 5a–d); and (ii) the contribution of mineral-bound sugars to MAOC overrode that of Fe-bound lignin after drainage (Fig. 4b). We infer that the following three potential processes may underlie these findings. First, wetland drainage and aeration may fuel the accumulation of microbial-derived carbon (including sugars; Fig. 3a and b; Jia et al., 2020; Chen et al., 2021) via increasing microbial activity (Fenner and Freeman, 2011), which contributed to MAOC due to microbial carbon's strong association with reactive Al and clay (Spielvogel et al., 2008; Mikutta et al., 2011; Dao et al., 2022). Second, mineral-bound fraction increased relative to total sugars in three out of four wetlands after drainage (Fig. S4e), suggesting that drainage may also promote mineral stabilization of (microbial-derived) sugars in the soil, likely due to stronger microbial attachment to mineral surfaces in unsaturated relative to saturated soils (Gargiulo et al., 2008; Pei et al., 2022). In unsaturated soils, microbes tend to attach to the mineral phase to access the thin water film to avoid dehydration (Mills, 2003; Kleber et al., 2015). Moreover, microbes may produce extracellular polysaccharides (good binding agents) to resist drought (Poli et al., 2011), which can also strengthen adherence between microbes and minerals (Ahimou et al., 2007; Hong et al., 2013). Third, in contrast to sugars, lignin phenols in bulk soils decreased (Fig. 3b) likely due to increasing microbial decomposition (indicated by decreased SOC:N; Fig. S5c) upon oxygen exposure, which could further decrease the formation of Fe-bound lignin phenols. Accordingly, Fe-bound lignin phenols decreased with decreasing SOC (Fig. S6a), decreasing SOC:N (Fig. 5g) as well as decreasing $Fe_o:Fe_d$ (Fig. 5e and S6b), suggesting that the overall decomposition of soil organic matter and crystallization of Fe (hydr)oxides likely hamper the preservation of Fe-bound lignin (Kleber et al., 2015; Hall et al., 2018).

As a result, mineral-bound sugars showed a relatively large increase in Fuyuan and Dajiuhu soils (Fig. 3d and S4d) that had notably increased

clay and Al_o contents (Fig. 2e and f) to stabilize microbial carbon after drainage (consistent with Hypothesis 2). However, Fe reactivity (indicated by $Fe_o:Fe_d$) decreased in Dajiuhu after drainage (Fig. 2d), likely due to the increase of Fe crystallinity via both decreasing organic matter and decreasing soil acidity after the replacement of *Sphagnum* (Chia-pusio et al., 2018; Fudyma et al., 2019; Zhao et al., 2021). Consequently, Fe-bound lignin phenols showed a considerable decrease in Dajiuhu (Fig. 3d and S4b), accompanied by an overall reduction of MAOC content at this site after drainage (Fig. 2h). However, it should be mentioned that the above processes need further validation by control experiments such as mesocosm water-table manipulation experiment. For example, observations of soil enzyme activity and microbial respiration may reflect changes in microbial activity upon oxygen exposure. The scanning electron microscopy (SEM) and nanoscale secondary ion mass spectrometry (nanoSIMS) can be employed to compare the attachment of microbial-derived components to mineral surfaces in saturated and unsaturated soils.

It should also be mentioned that despite an overall positive correlation between Fe-bound lignin phenols and Fe reactivity (i.e., $Fe_o:Fe_d$) in all soils (Fig. 5e and S6b), consistent with Hypothesis 3), drainage did not have a consistent effect on Fe reactivity or Fe-bound lignin phenols in all soils (Fig. 2d and 3c). Fe-bound lignin phenols increased in the air-exposed layers of Haibei wetland after the short-term drainage based on two-way ANOVA (Fig. S4b; Wang et al., 2017), despite unaltered $Fe_o:Fe_d$. It is speculated that the increased Fe-bound lignin phenols were mainly formed through coprecipitation or complexation rather than sorption during Fe oxidation upon aeration (Wang et al., 2017), and decreased soil pH due to Fe oxidation may have facilitated the association of Fe with lignin (Kleber et al., 2015; Wang et al., 2017). Similarly, many studies have found that a sizable fraction of SOC, especially aromatic and phenolic compounds, co-precipitated with newly formed Fe (hydr)oxides at the redox interface (Riedel et al., 2013; Hall et al., 2016; Huang et al., 2019; Li et al., 2022). The increase of Fe-bound lignin phenols was hence driven by elevated complexation (rather than sorption), and not necessarily by Fe reactivity changes. The duration of Fe-oxidation induced OC stabilization, however, awaits to be tested over longer timescales, because Fe-bound OC may be released via Fe reduction during redox fluctuations, as has been observed in incubation experiments (Huang and Hall, 2017), natural grasslands (Zhu et al., 2020) and permafrost-affected peatlands (Patzner et al., 2020). Prolonged exposure to oxygen may also increase the crystallinity and hence decrease the reactivity of Fe (hydr)oxides (Thompson et al., 2006), among other factors that regulate Fe transformation, such as dissolved organic matter (Thomas-Arrigo et al., 2018) and Fe-reducing or oxidizing microbes (Kappler et al., 2021). Hence, 'direct Fe protection of lignin' centered around Fe transformation did not seem to play a major role in carbon sequestration in the investigated wetlands subjected to long-term drainage (Dajiuhu, Hongyuan and Fuyuan). Moreover, as mentioned earlier, Fe-bound lignin quantified by the modified CuO oxidation method may be underestimated, because (1) lignin phenols are subjected to (presumably minor) loss, especially in SOC-lean samples (Fig. S6a), during the dithionite pretreatment (Shields et al., 2016; Wang et al., 2017; Jia et al., 2023; Zhu et al., 2023); and (2) lignin phenols only represent a fraction of the macromolecular lignin (Zakzeski et al., 2010; Ma et al., 2018). Therefore, the prevalence and persistence of the 'direct Fe protection of lignin' contributing to MAOC accrual still need to be examined in a wider range of long-term drainage sites, complemented by other analytical methods.

5. Conclusion and implications

In summary, our study shows that contrary to the common assumption about wetland SOC composition and response to drainage, MAOC made up a sizable fraction (7%–91%) of SOC and increased significantly in two out of three typical wetlands in China after decades of drainage. Moreover, using a novel analytical approach of quantifying

Fe-bound lignin phenols vs. mineral-bound (microbial) sugars, we compare the relative importance of 'direct Fe protection of lignin' vs. 'microbial processing' pathways governing MAOC dynamics after wetland drainage. It is found that mineral-bound sugars were predominantly derived from microbes and mainly associated with clay and reactive Al (i.e., Al_0), whereas Fe-bound lignin phenols increased with increasing Fe reactivity (i.e., Fe_0/Fe_d). After long-term drainage, MAOC increased with mineral-bound sugars, but decreased with Fe-bound lignin phenols in SOC. These results indicate that the microbial processing, involving stimulated microbial activity and enhanced mineral association of microbial-derived moieties, played a prominent role in wetland MAOC accumulation after long-term drainage, especially in soils rich in reactive Al and clay. By comparison, the 'direct Fe protection of lignin', mainly mediated by Fe trapping of carbon (such as lignin) during Fe oxidation, was only observed in a wetland experiencing short-term drainage, and may be undermined by Fe reduction and crystallization during redox fluctuations in the long term. In all, our study highlights a prominent microbial regulation on MAOC accrual in wetlands after drainage, an under-investigated process compared to upland soils. Given the long turnover of MAOC, its increase may partly compensate for POC loss due to increased decomposition during wetland drainage, and be key to wetland SOC stabilization in the long term. However, it should be mentioned that the responses of MAOM or Fe-bound OC to drainage may vary across different types of wetlands with different vegetation, climatic and edaphic characteristics. Therefore, the prevalence and persistence of the 'direct Fe protection of lignin' and 'microbial processing' pathways contributing to MAOC accrual await to be examined in a wider range of wetlands, ideally using complementary approaches to those employed here, such as microscale spectroscopy and analytical pyrolysis that do not involve chemical extractions.

Declaration of competing interest

The authors declare that they have no known competing financial interests or personal relationships that could have appeared to influence the work reported in this paper.

Data availability

Data will be made available on request.

Acknowledgements

The study was financially supported by the National Natural Science Foundation of China (42230501, 31988102, 42025303). We thank the Plant Science Facility of the Institute of Botany, Chinese Academy of Sciences for bulk soil analysis. The authors have no conflict of interest to declare.

Appendix A. Supplementary data

Supplementary data to this article can be found online at <https://doi.org/10.1016/j.soilbio.2023.109152>.

References

Ahimou, F., Semmens, M.J., Haugstad, G., Novak, P.J., 2007. Effect of protein, polysaccharide, and oxygen concentration profiles on biofilm cohesiveness. *Applied and Environmental Microbiology* 73, 2905–2910.

Anthony, T.L., Silver, W.L., 2020. Mineralogical associations with soil carbon in managed wetland soils. *Global Change Biology* 26, 6555–6567.

Bai, J., Luo, M., Yang, Y., Xiao, S.Y., Zhai, Z.F., Huang, J.F., 2021. Iron-bound carbon increases along a fresh water oligohaline gradient in a subtropical tidal wetland. *Soil Biology and Biochemistry* 154, 108128.

Bhattacharyya, A., Schmidt, M.P., Stavitski, E., Martínez, C.E., 2018. Iron speciation in peats: chemical and spectroscopic evidence for the co-occurrence of ferric and

ferrous iron in organic complexes and mineral precipitates. *Organic Geochemistry* 115, 124–137.

Blume, H.P., Schwertmann, U., 1969. Genetic evaluation of profile distribution of aluminum, iron, and manganese oxides. *Soil Science Society of America Journal* 33, 438–444.

Chen, C.M., Dynes, J.J., Wang, J., Sparks, D.L., 2014. Properties of Fe-organic matter associations via coprecipitation versus adsorption. *Environmental Science and Technology* 48, 13751–13759.

Chen, X.B., Hu, Y.J., Xia, Y.H., Zheng, S.M., Ma, C., Rui, Y.C., He, H.B., Huang, D.Y., Zhang, Z.H., Ge, T.D., Wu, J.S., Guggenberger, G., Kuzyakov, Y., Su, Y.R., 2021. Contrasting pathways of carbon sequestration in paddy and upland soils. *Global Change Biology* 27, 2478–2490.

Chiapusio, G., Jassey, V.E.J., Bellvert, F., Comte, G., Weston, L.A., Delarue, F., Buttler, A., Toussaint, M.L., Binet, P., 2018. Sphagnum species modulate their phenolic profiles and mycorrhizal colonization of surrounding *Andromeda polifolia* along peatland microhabitats. *Journal of Chemical Ecology* 44, 1146–1157.

Cotrufo, M.F., Wallenstein, M.D., Boot, C.M., Denef, K., Paul, E., 2013. The Microbial Efficiency-Matrix Stabilization (MEMS) framework integrates plant litter decomposition with soil organic matter stabilization: do labile plant inputs form stable soil organic matter? *Global Change Biology* 19, 988–995.

Coward, E.K., Ohno, T., Plante, A.F., 2018. Adsorption and molecular fractionation of dissolved organic matter on iron-bearing mineral matrices of varying crystallinity. *Environmental Science and Technology* 52, 1036–1044.

Creamer, C.A., Foster, A.L., Lawrence, C., McFarland, J., Schulz, M., Waldrop, M.P., 2019. Mineralogy dictates the initial mechanism of microbial necromass association. *Geochimica et Cosmochimica Acta* 260, 161–176.

Dahlgren, R.A., 1994. Quantification of allophane and imogolite. In: Amonette, J.E., Stucki, J.W. (Eds.), *Quantitative Methods in Soil Mineralogy*. Soil Science Society of America Journal, pp. 430–451.

Dao, T.T., Mikutta, R., Sauheitl, L., Gentsch, N., Shibistova, O., Wild, B., Schnecker, J., Bárta, J., Čapek, P., Gittel, A., Lashchinskiy, N., Ulrich, T., Santrůčková, H., Richter, A., Guggenberger, G., 2022. Lignin preservation and microbial carbohydrate metabolism in permafrost soils. *Journal of Geophysical Research: Biogeosciences* 127, 1–22.

Davidson, N.C., Fluet-Chouinard, E., Finlayson, C.M., 2018. Global extent and distribution of wetlands: trends and issues. *Marine and Freshwater Research* 69, 620–627.

Evans, C.D., Peacock, M., Baird, A.J., Artz, R.R.E., Burden, A., Callaghan, N., Chapman, P.J., Cooper, H.M., Coyle, M., Craig, E., Cumming, A., Dixon, S., Gauci, V., Grayson, R.P., Helfter, C., Heppell, C.M., Holden, J., Jones, D.L., Kaduk, J., Levy, P., Matthews, R., McNamara, N.P., Misselbrook, T., Oakley, S., Page, S., Rayment, M., Ridley, L.M., Stanley, K.M., Williamson, J.L., Worrall, F., Morrison, R., 2021. Overriding water table control on managed peatland greenhouse gas emissions. *Nature* 593, 548–552.

Feng, X.J., Simpson, M.J., 2008. Temperature responses of individual soil organic matter components. *Journal of Geophysical Research: Biogeosciences* 113, G03036.

Fenner, N., Freeman, C., 2011. Drought-induced carbon loss in peatlands. *Nature Geoscience* 4, 895–900.

Fluet-Chouinard, E., Stocker, B.D., Zhang, Z., Malhotra, A., Melton, J.R., Poulter, B., Kaplan, J.O., Goldewijk, K.K., Siebert, S., Minayeva, T., 2023. Extensive global wetland loss over the past three centuries. *Nature* 614, 281–286.

Freeman, C., Ostle, N., Kang, H., 2001. An enzymic 'latch' on a global carbon store - a shortage of oxygen locks up carbon in peatlands by restraining a single enzyme, 149–149 *Nature* 409.

Fudyma, J.D., Lyon, J., AminiTabrizi, R., Gieschen, H., Chu, R.K., Hoyt, D.W., Kyle, J.E., Toyoda, J., Tolic, N., Heyman, H.M., Hess, N.J., Metz, T.O., Tfaily, M.M., 2019. Untargeted metabolomic profiling of *Sphagnum fallax* reveals novel antimicrobial metabolites. *Plant Direct* 3, 1–17.

Gargiulo, G., Bradford, S.A., Simunek, J., Ustohal, P., Vereecken, H., Klumpp, E., 2008. Bacteria transport and deposition under unsaturated flow conditions: the role of water content and bacteria surface hydrophobicity. *Vadose Zone Journal* 7, 406–419.

Georgiou, K., Jackson, R.B., Vinduskova, O., Abramoff, R.Z., Ahlstrom, A., Feng, W., Harden, J.W., Pellegrini, A.F.A., Polley, H.W., Soong, J.L., Riley, W.J., Torn, M.S., 2022. Global stocks and capacity of mineral-associated soil organic carbon. *Nature Communications* 13, 3797.

Griepentrog, M., Bode, S., Boeckx, P., Hagedorn, F., Heim, A., Schmidt, M.W., 2014. Nitrogen deposition promotes the production of new fungal residues but retards the decomposition of old residues in forest soil fractions. *Global Change Biology* 20, 327–340.

Gunina, A., Kuzyakov, Y., 2015. Sugars in soil and sweets for microorganisms: review of origin, content, composition and fate. *Soil Biology and Biochemistry* 90, 87–100.

Hall, S.J., Thompson, A., 2021. What do relationships between extractable metals and soil organic carbon concentrations mean? *Soil Science Society of America Journal* 86, 1–14.

Hall, S.J., Silver, W.L., Timokhin, V.I., Hammel, K.E., 2016. Iron addition to soil specifically stabilized lignin. *Soil Biology and Biochemistry* 98, 95–98.

Hall, S.J., Berhe, A.A., Thompson, A., 2018. Order from disorder: do soil organic matter composition and turnover co-vary with iron phase crystallinity? *Biogeochemistry* 140, 93–110.

Han, L.F., Yang, Y., Sun, K., Zhang, B., Chen, Y.L., Fang, L.P., Xing, B.S., 2021. Different mechanisms driving the preferential adsorption of dissolved organic matter by goethite and montmorillonite. *Chemical Geology* 585, 120560.

Harris, D., Horwath, W.R., van Kessel, C., 2001. Acid fumigation of soils to remove carbonates prior to total organic carbon or carbon-13 isotopic analysis. *Soil Science Society of America Journal* 65, 1853–1856.

- Heckman, K., Hicks Pries, C.E., Lawrence, C.R., Rasmussen, C., Crow, S.E., Hoyt, A.M., von Fromm, S.F., Shi, Z., Stoner, S., McGrath, C., Beem-Miller, J., Berhe, A.A., Blankinship, J.C., Keiluweit, M., Marin-Spiotta, E., Monroe, J.G., Plante, A.F., Schimel, J., Sierra, C.A., Thompson, A., Wagai, R., 2022. Beyond bulk: density fractions explain heterogeneity in global soil carbon abundance and persistence. *Global Change Biology* 28, 1178–1196.
- Hedges, J.I., Cowie, G.L., Ertel, J.R., Barbour, R.J., Hatcher, P.G., 1985. Degradation of carbohydrates and lignins in buried woods. *Geochimica et Cosmochimica Acta* 49, 701–711.
- Hedges, L.V., Gurevitch, J., Curtis, P.S., 1999. The meta-analysis of response ratios in experimental ecology. *Ecology* 80, 1150–1156.
- Hong, Z., Chen, W., Rong, X., Cai, P., Dai, K., Huang, Q., 2013. The effect of extracellular polymeric substances on the adhesion of bacteria to clay minerals and goethite. *Chemical Geology* 360–361, 118–125.
- Hothorn, T., Bretz, F., Westfall, P., 2008. Simultaneous inference in general parametric models. *Biometrical Journal: Journal of Mathematical Methods in Biosciences* 50, 346–363.
- Huang, W., Hall, S.J., 2017. Elevated moisture stimulates carbon loss from mineral soils by releasing protected organic matter. *Nature Communications* 8, 1774. <https://doi.org/10.1038/s41467-017-01998-z>.
- Huang, W.J., Hammel, K.E., Hao, J., Thompson, A., Timokhin, V.I., Hall, S.J., 2019. Enrichment of lignin-derived carbon in mineral-associated soil organic matter. *Environmental Science and Technology* 53, 7522–7531.
- Huang, Y.Y., Ciais, P., Luo, Y.Q., Zhu, D., Wang, Y.P., Qiu, C.J., Goll, D.S., Guenet, B., Makowski, D., De Graaf, I., Leifeld, J., Kwon, M.J., Hu, J., Qu, L.Y., 2021a. Tradeoff of CO₂ and CH₄ emissions from global peatlands under water-table drawdown. *Nature Climate Change* 11, 618–622.
- Huang, X.Y., Liu, X.W., Liu, J.L., Chen, H., 2021b. Iron-bound organic carbon and their determinants in peatlands of China. *Geoderma* 391, 114974.
- Ji, H., Han, J.G., Xue, J.M., Hatten, J.A., Wang, M.H., Guo, Y.H., Li, P.P., 2020. Soil organic carbon pool and chemical composition under different types of land use in wetland: implication for carbon sequestration in wetlands. *The Science of the Total Environment* 716, 136996.
- Jia, B., Niu, Z.Q., Wu, Y.N., Kuzyakov, Y., Li, X.G., 2020. Waterlogging increases organic carbon decomposition in grassland soils. *Soil Biology and Biochemistry* 148, 107927.
- Jia, J., Liu, Z., Haghipour, N., Wacker, L., Zhang, H., Sierra, C.A., Ma, T., Wang, Y., Chen, L., Luo, A., Wang, Z., He, J., Zhao, M., Eglinton, T.I., Feng, X., 2023. Molecular ¹⁴C evidence for contrasting turnover and temperature sensitivity of soil organic matter components. *Ecology Letters* 26, 778–788.
- Kaiser, K., 2003. Sorption of natural organic matter fractions to goethite, α -Fe(OH)₃: effect of chemical composition as revealed by liquid-state ¹³C NMR and wet-chemical analysis. *Organic Geochemistry* 34, 1569–1579.
- Kappler, A., Bryce, C., Mansor, M., Lueder, U., Byrne, J.M., Swanner, E.D., 2021. An evolving view on biogeochemical cycling of iron. *Nature Reviews Microbiology* 19, 360–374.
- Kiem, R., Kögel-Knabner, I., 2003. Contribution of lignin and polysaccharides to the refractory carbon pool in C-depleted arable soils. *Soil Biology and Biochemistry* 35, 101–118.
- Kleber, M., Eusterhues, K., Keiluweit, M., Mikutta, C., Mikutta, R., Nico, P.S., 2015. Mineral-organic associations: formation, properties, and relevance in soil environments. *Advances in Agronomy* 130, 1–140.
- Kögel-Knabner, I., 2002. The macromolecular organic composition of plant and microbial residues as inputs to soil organic matter. *Soil Biology and Biochemistry* 34, 139–162.
- Kopittke, P.M., Hernandez-Soriano, M.C., Dalal, R.C., Finn, D., Menzies, N.W., Hoeschen, C., Mueller, C.W., 2018. Nitrogen-rich microbial products provide new organo-mineral associations for the stabilization of soil organic matter. *Global Change Biology* 24, 1762–1770.
- Kramer, M.G., Sanderman, J., Chadwick, O.A., Chorover, J., Vitousek, P.M., 2012. Long-term carbon storage through retention of dissolved aromatic acids by reactive particles in soil. *Global Change Biology* 18, 2594–2605.
- Lalonde, K., Mucci, A., Ouellet, A., Gelinis, Y., 2012. Preservation of organic matter in sediments promoted by iron. *Nature* 483, 198–200.
- Lavallee, J.M., Soong, J.L., Cotrufo, M.F., 2020. Conceptualizing soil organic matter into particulate and mineral-associated forms to address global change in the 21st century. *Global Change Biology* 26, 261–273.
- Lee, H., Galy, V., Feng, X.J., Ponton, C., Galy, A., France-Lanord, C., Feakins, S.J., 2019. Sustained wood burial in the bengal fan over the last 19 my. *Proceedings of the National Academy of Sciences of the United States of America* 116, 22518–22525.
- Leifeld, J., Wüst-Galley, C., Page, S., 2019. Intact and managed peatland soils as a source and sink of GHGs from 1850 to 2100. *Nature Climate Change* 9, 945–947.
- Li, Y., Chen, Z.M., Chen, J., Castellano, M.J., Ye, C.L., Zhang, N., Miao, Y.C., Zheng, H.J., Li, J.J., Ding, W.X., 2022. Oxygen availability regulates the quality of soil dissolved organic matter by mediating microbial metabolism and iron oxidation. *Global Change Biology* 28, 7410–7427.
- Liang, C., Schimel, J.P., Jastrow, J.D., 2017. The importance of anabolism in microbial control over soil carbon storage. *Nature Microbiology* 2, 17105.
- Liu, C.Z., Wang, S.M., Zhu, E.X., Jia, J., Zhao, Y.P., Feng, X.J., 2021. Long-term drainage induces divergent changes of soil organic carbon contents but enhances microbial carbon accumulation in fen and bog. *Geoderma* 404, 115343.
- Louchouart, P., Opsahl, S., Benner, R., 2000. Isolation and quantification of dissolved lignin from natural waters using solid-phase extraction and GC/MS. *Analytical Chemistry* 72, 2780–2787.
- Lu, M.Z., Zou, Y.C., Xun, Q.L., Yu, Z.C., Jiang, M., Sheng, L.X., Lu, X.G., Wang, D.L., 2021. Anthropogenic disturbances caused declines in the wetland area and carbon pool in China during the last four decades. *Global Change Biology* 27, 3837–3845.
- Ma, T., Zhu, S.S., Wang, Z.H., Chen, D.M., Dai, G.H., Feng, B.W., Su, X.Y., Hu, H.F., Li, K. H., Han, W.X., Liang, C., Bai, Y.F., Feng, X.J., 2018. Divergent accumulation of microbial necromass and plant lignin components in grassland soils. *Nature Communications* 9, 3480.
- Mikutta, R., Schaumann, G.E., Gildemeister, D., Bonneville, S., Kramer, M.G., Chorover, J., Chadwick, O.A., Guggenberger, G., 2009. Biogeochemistry of mineral-organic associations across a long-term mineralogical soil gradient, 0.3–4100kyr, Hawaiian Islands. *Geochimica et Cosmochimica Acta* 73, 2034–2060.
- Mikutta, R., Zang, U., Chorover, J., Haumaier, L., Kalbitz, K., 2011. Stabilization of extracellular polymeric substances, *Bacillus subtilis* by adsorption to and coprecipitation with Al forms. *Geochimica et Cosmochimica Acta* 75, 3135–3154.
- Mills, A.L., 2003. Keeping in touch: microbial life on soil particle surfaces. *Advances in Agronomy* 78, 2–45.
- Oades, J.M., 1984. Soil organic matter and structural stability: mechanisms and implications for management. *Plant and Soil* 76, 319–337.
- Parfitt, R., Childs, C., 1988. Estimation of forms of Fe and Al - a review, and analysis of contrasting soils by dissolution and Mossbauer methods. *Soil Research* 26, 121–144.
- Patzner, M.S., Mueller, C.W., Malusova, M., Baur, M., Nikeleit, V., Scholten, T., Hoeschen, C., Byrne, J.M., Borch, T., Kappler, A., Bryce, C., 2020. Iron mineral dissolution releases iron and associated organic carbon during permafrost thaw. *Nature Communications* 11, 6329.
- Pei, H., Yang, H., Kuzyakov, Y., Dang, X., Zang, J., Zhao, S., Huang, M., Wang, C., Xie, S., 2022. Archaeal lipids in soils and sediments: water impact and consequences for microbial carbon sequestration. *Soil Biology and Biochemistry* 173, 108801.
- Pinheiro, J., Bates, D., DebRoy, S., Sarkar, D., R Core Team, 2020. *Nlme: Linear and Nonlinear Mixed Effects Models*. R Package Version 3.1-148. URL: <https://CRAN.R-project.org/package=nlme>.
- Poli, A., Di Donato, P., Abbamondi, G.R., Nicolaus, B., 2011. Synthesis, production, and biotechnological applications of exopolysaccharides and polyhydroxyalkanoates by archaea. *Archaea* 2011, 693253.
- Rennett, T., 2019. Wet-chemical extractions to characterise pedogenic Al and Fe species - a critical review. *Soil Research* 57, 1–16.
- Riedel, T., Biester, H., Dittmar, T., 2012. Molecular fractionation of dissolved organic matter with metal salts. *Environmental Science and Technology* 46, 4419–4426.
- Riedel, T., Zak, D., Biester, H., Dittmar, T., 2013. Iron traps terrestrially derived dissolved organic matter at redox interfaces. *Proceedings of the National Academy of Sciences of the United States of America* 110, 10101–10105.
- Rumpel, C., Eusterhues, K., Kögel-Knabner, I., 2010. Non-cellulosic neutral sugar contribution to mineral associated organic matter in top- and subsoil horizons of two acid forest soils. *Soil Biology and Biochemistry* 42, 379–382.
- Ryzak, M., Bieganski, A., 2011. Methodological aspects of determining soil particle-size distribution using the laser diffraction method. *Journal of Plant Nutrition and Soil Science* 174, 624–633.
- Shields, M.R., Bianchi, T.S., Gelinis, Y., Allison, M.A., Twilley, R.R., 2016. Enhanced terrestrial carbon preservation promoted by reactive iron in deltaic sediments. *Geophysical Research Letters* 43, 1149–1157.
- Sokol, N.W., Bradford, M.A., 2019. Microbial formation of stable soil carbon is more efficient from belowground than aboveground input. *Nature Geoscience* 12, 46–53.
- Sokol, N.W., Sanderman, J., Bradford, M.A., 2019. Pathways of mineral-associated soil organic matter formation: integrating the role of plant carbon source, chemistry, and point of entry. *Global Change Biology* 25, 12–24.
- Sokol, N.W., Whalen, E.D., Jilling, A., Kallenbach, C., Pett-Ridge, J., Georgiou, K., 2022. Global distribution, formation, and fate of mineral-associated soil organic matter under a changing climate—a trait-based perspective. *Functional Ecology* 3, 1411–1429.
- Souto, F., Calado, V., Pereira, N., 2018. Lignin-based carbon fiber: a current overview. *Materials Research Express* 5, 072001.
- Spencer, R.G.M., Aiken, G.R., Dyda, R.Y., Butler, K.D., Bergamaschi, B.A., Hernes, P.J., 2010. Comparison of XAD with other dissolved lignin isolation techniques and a compilation of analytical improvements for the analysis of lignin in aquatic settings. *Organic Geochemistry* 41, 445–453.
- Spielvogel, S., Prietzel, J., Kögel-Knabner, I., 2008. Soil organic matter stabilization in acidic forest soils is preferential and soil type-specific. *European Journal of Soil Science* 59, 674–692.
- Temmink, R.J.M., Lamers, L.P.M., Angelini, C., Bouma, T.J., Fritz, C., van de Koppel, J., Loxmond, R., Rietkerk, M., Silliman, B.R., Joosten, H., van der Heide, T., 2022. Recovering wetland biogeomorphic feedbacks to restore the world's biotic carbon hotspots. *Science* 376, eabn1479.
- ThomasArrigo, L.K., Byrne, J.M., Kappler, A., Kretzschmar, R., 2018. Impact of organic matter on iron(II)-catalyzed mineral transformations in ferrihydrite-organic matter coprecipitates. *Environmental Science and Technology* 52, 12316–12326.
- Thompson, A., Chadwick, O.A., Rancourt, D.G., Chorover, J., 2006. Iron-oxide crystallinity increases during soil redox oscillations. *Geochimica et Cosmochimica Acta* 70, 1710–1727.
- Turetsky, M.R., Donahue, W.F., Benscoter, B.W., 2011. Experimental drying intensifies burning and carbon losses in a northern peatland. *Nature Communications* 2, 514.
- Wang, Q., Zhang, P.-J., Liu, M., Deng, Z.-W., 2014. Mineral-associated organic carbon and black carbon in restored wetlands. *Soil Biology and Biochemistry* 75, 300–309.
- Wang, Y.Y., Wang, H., He, J.-S., Feng, X.J., 2017. Iron-mediated soil carbon response to water-table decline in an alpine wetland. *Nature Communications* 8, 15972.
- Wang, S.M., Jia, Y.F., Liu, T., Wang, Y.Y., Liu, Z.G., Feng, X.J., 2021. Delineating the role of calcium in the large-scale distribution of metal-bound organic carbon in soils. *Geophysical Research Letters* 48, e2021GL029391.
- Wang, Y., Wang, S., Liu, C., Zhu, E., Jia, J., Feng, X., 2023. Shifting relationships between SOC and molecular diversity in soils of varied carbon concentrations: evidence from drained wetlands. *Geoderma* 433, 116459.

- Wei, L., Zhu, Z.K., Razavi, B.S., Xiao, M.L., Dorodnikov, M., Fan, L.C., Yuan, H.Z., Yurtaev, A., Luo, Y., Cheng, W.G., Kuzyakov, Y., Wu, J.S., Ge, T.D., 2022. Visualization and quantification of carbon “rusty sink” by rice root iron plaque: mechanisms, functions, and global implications. *Global Change Biology* 00, 1–17.
- Ye, C.L., Chen, D.M., Hall, S.J., Pan, S., Yan, X.B., Bai, T.S., Guo, H., Zhang, Y., Bai, Y.F., Hu, S.J., 2018. Reconciling multiple impacts of nitrogen enrichment on soil carbon: plant, microbial and geochemical controls. *Ecology Letters* 21, 1162–1173.
- Younes, K., Laduranty, J., Descostes, M., Grasset, L., 2017. Molecular biomarkers study of an ombrotrophic peatland impacted by an anthropogenic clay deposit. *Organic Geochemistry* 105, 20–32.
- Yu, Z.C., Loisel, J., Brosseau, D.P., Beilman, D.W., Hunt, S.J., 2010. Global peatland dynamics since the last glacial maximum. *Geophysical Research Letters* 37, L13402.
- Zakzeski, J., Bruijninx, P.C.A., Jongerius, A.L., Weckhuysen, B.M., 2010. The catalytic valorization of lignin for the production of renewable chemicals. *Chemical Reviews* 110, 3552–3599.
- Zedler, J.B., Kercher, S., 2005. Wetland resources: status, trends, ecosystem services, and restorability. *Annual Review of Environment and Resources* 30, 39–74.
- Zhang, W., He, H.B., Zhang, X.D., 2007. Determination of neutral sugars in soil by capillary gas chromatography after derivatization to aldonitrile acetates. *Soil Biology and Biochemistry* 39, 2665–2669.
- Zhao, Y.P., Xiang, W., Ma, M., Zhang, X.Z., Bao, Z.Y., Xie, S.Y., Yan, S., 2019. The role of laccase in stabilization of soil organic matter by iron in various plant-dominated peatlands: degradation or sequestration? *Plant and Soil* 443, 575–590.
- Zhao, Y.P., Liu, C.Z., Wang, S.M., Wang, Y.Y., Liu, X.Q., Luo, W.Q., Feng, X.J., 2021. Triple locks’ on soil organic carbon exerted by sphagnum acid in wetlands. *Geochimica et Cosmochimica Acta* 315, 24–37.
- Zhu, E.X., Liu, Z.G., Wang, S.M., Wang, Y., Liu, T., Feng, X.J., 2023. Organic carbon and lignin protection by metal oxides versus silicate clay: Comparative study based on wetland and upland soils. *Journal of Geophysical Research: Biogeosciences* 128 e2023JG007474.
- Zhu, E.X., Liu, T., Zhou, L., Wang, S.M., Wang, X., Zhang, Z.H., Wang, Z.W., Bai, Y.F., Feng, X.J., 2020. Leaching of organic carbon from grassland soils under anaerobiosis. *Soil Biology and Biochemistry* 141, 107684.